LWT - Food Science and Technology 159 (2022) 113211

Contents lists available at ScienceDirect

LWT

journal homepage: www.elsevier.com/locate/lwt

Pathogenic mono-species biofilm formation on stainless steel surfaces: Quantitative, qualitative, and compositional study

B.R.H. Cervantes-Huamán, C. Ripolles-Avila *, T. Mazaheri, J.J. Rodríguez-Jerez

Area of Human Nutrition and Food Science, Departament de Ciència Animal i dels Aliments, Facultat de Veterinària, Universitat Autònoma de Barcelona, Bellaterra (Cerdanyola del Vallès), CP 08193, Barcelona, Spain

ARTICLE INFO

Keywords:
Surface hygiene
Foodborne pathogens
Biofilms
DEM
CLSM

ABSTRACT

The aims of this study were, first, to determine *Listeria monocytogenes*, *Salmonella enterica,* ser. Typhimurium, and *Staphylococcus aureus* biofilm counts, structure, and their composition in macromolecules by direct epifluorescence microscopy (DEM); and second, to evaluate the distribution of the components of the produced biofilms through 3D representations obtained by confocal laser scanning microscopy (CLSM). Results showed that all assessed strains have a high capacity to generate biofilms, with counts greater than 7 log CFU cm^{-2} in all cases. The highest and lowest survival percentages were obtained by *S. aureus* with 94.13 ± 1.77% and *S.* Typhimurium with 60.31 ± 4.45%, respectively. Biofilm matrix composition in macromolecules was as follows: (a) *L. monocytogenes*: proteins 83.35 ± 5.81%, polysaccharides 10.98 ± 5.77%, and extracellular DNA 5.67 ± 2.5%; (b) *S.* Typhimurium: 83.37 ± 3.35%, 0.68 ± 0.77%, and 15.95 ± 3.39%, respectively; and (c) *S. aureus*: 82.55 ± 2.39%, 8.48 ± 2.07%, and 8.97 ± 2.27%, respectively. The qualitative analysis of the 3D representations of the biofilms formed by the pathogens modelized showed no homogeneity and/or ordered distribution of their components within the biofilm architecture. These findings could lead to the development of addressed cleaning and disinfection alternatives.

1. Introduction

The formation of biofilms by pathogenic bacteria on food contact surfaces is one of the main problems faced by the food industry given that this not only puts consumers' health at risk, but it is also an important cause of reduced economic productivity (OMS, 2015). According to the National Institutes of Health (NIH) and the Centers for Disease Control and Prevention (CDC), biofilms are involved in more than 65% of foodborne illnesses. It is currently well documented that food pathogens such as *Listeria monocytogenes*, *Salmonella* spp., and *Staphylococcus aureus* can produce biofilms on work surfaces and facilities, making them leading causes of outbreaks due to cross-contamination to the final product (Dantas et al., 2018). These three microorganisms present high mortality and incidence rates in Europe and E.E.U.U., respectively. Biofilms are complex microbial communities, irreversibly attached to a surface and embedded in a matrix of self-produced extracellular components (ECM), which exhibit an altered phenotype in relation to the rate of growth and gene transcription of planktonic cells (González-Rivas et al., 2018). The ECM produced consists mainly of polysaccharides, proteins, and extracellular DNA (eDNA) (Jahid & Ha, 2012), and in smaller quantities products from bacterial lysis (Branda et al., 2005). Most microorganisms are considered capable of forming biofilms under suitable environmental conditions (Lasa et al., 2005). This capacity represents an adaptive and resistance strategy for microorganisms, allowing them to increase the availability of nutrients for their growth, facilitate the use of water or even enable the transfer of genetic material. This, in fact, is what is most worrying for the food industry, as biofilms can confer to bacterial cells resistance against antimicrobial agents (González-Rivas et al., 2018). Consequently, routine cleaning and disinfection operations are often ineffective against the bacteria that form biofilms (Møretrø et al., 2013).

It has been reported that 99% of all bacterial cells exist as biofilms and that only 1% is in a planktonic state (Ramadan, 2006), providing sufficient reason to continue investigating this predominant form at the microbial level. In this regard, only the presence of a hydrated environment and a minimum amount of nutrients are required to originate biofilm formation (Terry et al., 2003), factors that are continuously present in the food industry. The biofilm development process is multifactorial and consists of 5 stages: (i) reversible adhesion to the surface; (ii) irreversible adhesion through the production of ECM and *quorum sensing*; (iii) formation of microcolonies; (iv)

* Corresponding author.
E-mail address: carolina.ripolles@uab.cat (C. Ripolles-Avila).

https://doi.org/10.1016/j.lwt.2022.113211
Received 6 October 2021; Received in revised form 26 December 2021; Accepted 5 February 2022
Available online 8 February 2022

maturation; and (v) dispersion (Jahid & Ha, 2012; Srey et al., 2013). Once biofilms are formed on a surface, the cells present in the structure can be between 500 and 1500 times more resistant to biocides than planktonic cells (Hyde et al., 1998), due to the protective matrix (Carpentier & Cerf, 2011). Furthermore, biofilm cells are more resistant to high temperatures, low pH (Castro-Rosas & Escartín, 2005), desiccation, UV rays, and salinity, making their removal more difficult (Speranza et al., 2016). This resistance can allow the persistence of biofilm cells in the food industry, constituting a continuous source of microbial contamination (Poimenidou et al., 2016). Thus, it is important to have effective cleaning and disinfection procedures, which implies the suitable selection of the products used for this purpose (Ripolles-Avila, Hascoët, et al., 2019). Among them, enzymatic products stand out, having been shown to partially or totally degrade biofilm matrices (Coughlan et al., 2016; Mazaheri et al., 2020; Ripolles-Avila, Hascoët, et al., 2019). These detergents combined with other disinfecting treatments improve biofilm removal and elimination (Meireles et al., 2016), which explains why understanding the composition in macromolecules of microbial biofilms enables enzymatic products to be designed according to the type of matrix produced by the dominant pathogenic microbiota in each food industry.

The main objectives of the present study were first to determine the biofilm formation capacity and composition in macromolecules of *L. monocytogenes* CECT 5672, *S.* Typhimurium CECT 4594, and *S. aureus* CECT 239 as representative pathogenic models, using direct epifluorescence microscopy (DEM); and second, to evaluate the distribution and architecture of the matrix components of the formed biofilms through 3D representations obtained by confocal laser scanning microscopy (CLSM).

2. Materials and methods

2.1. Test surfaces

AISI 316 grade 2B stainless steel coupons (2 cm in diameter and 1 mm thick) were used in this study. Prior to use, they were subjected to cleaning and disinfection procedures. The procedure started with cleaning the surfaces by immersing them in an aqueous solution with a non-bactericidal detergent for 1 h (ADIS Hygiene, Madrid, Spain). The surfaces were then washed three times with distilled water for 10 s, subsequently disinfected with 70% isopropanol (Panreac Química, Castellar del Vallès, Spain), and dried in a laminar flow cabinet (PV-30/70, Telstar, Terrassa, Spain), all according to European standard UNE-EN 13697:2015 regarding non-porous materials (AENOR, 2015). Last, the surfaces were autoclaved for 15 min at 121 °C to ensure their sterility before starting the tests.

2.2. Bacterial strains

L. monocytogenes CECT 5672, *S.* Typhimurium CECT 4594, and *S. aureus* CECT 239 were obtained as freeze-dried cultures from the Spanish Type Culture Collection (CECT, University of Valencia, Valencia, Spain). These freeze-dried cultures were rehydrated in Tryptic Soy Broth (TSB; Oxoid, Madrid, Spain) for 48 h at 30 °C, and then cultured on Tryptic Soy Agar (TSA; Oxoid, Madrid, Spain) for 48 h at 30 °C. Isolated colonies were used to prepare stock cultures on TSA slants, which were incubated for 24 h at 37 °C and stored for up to 1 month at 4 °C.

2.3. Inoculum preparation

The bacterial inoculum was prepared by culturing the stock bacterial strains overnight in TSA at 37 °C. Several colonies obtained on the TSA were then inoculated to $TSYEB_{gluc1\%+NaCl2\%}$ [consisting of TSB supplemented with 0.3% w/v yeast extract (BD, Madrid, Spain), 1% w/v glucose (BioLife, Barcelona, Spain), and 2% w/v sodium chloride (Panreac, Castellar del Vallès, Spain)] for *L. monocytogenes,* and to TSB for *S.* Typhimurium and *S. aureus,* until an approximate concentration of 10^6 CFU ml^{-1} was obtained using a densitometer (DENSIMAT, bioMérieux, Marcy l'Etoile, France).

2.4. Mono-species biofilm formation on stainless steel surfaces

This process was carried out following the *in vitro* biofilm formation model established by Ripolles-Avila et al. (2018). For this, 30 μl of the bacterial inoculum, described in section 2.3, were inoculated in the center of each stainless-steel coupon. The coupons were put into sterile Petri dishes and subsequently placed in a humidity chamber maintained at saturated relative humidity of >90% and incubated at 30 °C to promote biofilm growth under moist conditions (Fuster-Valls et al., 2008). The biofilms were formed in static conditions for a week, with washings and nutrient renewal established at 2, 3, 6, and 7 days of incubation. To this effect, 6 ml of sterile distilled water was used to wash each coupon, while 30 μl of $TSYEB_{gluc1\%+NaCl2\%}$ was used for nutrient renewal for *L. monocytogenes,* and TSB was used for *S.* Typhimurium and *S. aureus*.

2.5. Evaluation of the biofilm formation capacity by DEM

After the incubation period, the surfaces were washed with 6 ml of sterile distilled water to remove all the cells that did not adhere to the surface and were therefore not part of the generated biofilm. Subsequently, the coupons were stained with 5 μl of Live/Dead BacLight bacterial viability kit (Molecular Probes, Oregon, USA) and incubated at room temperature in dark conditions for 15 min. The kit is composed of two fluorescent nucleic acid-binding stains, SYTO9 and propidium iodide. The first fluorochrome labels all cells, both damaged and intact membranes, while the second only penetrates cells with damaged membranes, causing a reduction of the first dye. To this effect, viable cells with an intact membrane appear in fluorescent green, while dead or damaged cells appear in fluorescent red.

After incubation, the coupons were evaluated by DEM, using an Olympus BX51/BX52 direct epifluorescence microscope (Olympus, Tokyo, Japan) equipped with a 100 W mercury lamp (USH-103OL, Olympus) and a double pass filter cube (U-M51004 F/R–V2, Olympus), and coupled to a digital camera (DP73, Olympus). The surfaces were observed with a 20X objective. To determine the number of viable and non-viable cells in each sample, 6 random pictures of 6 separate fields, equating to 0.16 mm^2, were taken, from which an estimate of the number of cells per square centimeter was obtained. The image analysis was carried out using Auto 3.2 software (Soft Imaging System GMBH, Münster, Germany). The means of the cell area and the biofilm occupied area in each image were thereby obtained. The total number of cells was calculated by dividing the average surface occupied by the biofilm by the area of the cells (Ripolles-Avila, Ríos-Castillo, et al., 2019). The results were expressed as the logarithm of the number of colony-forming units (CFU) per square centimeter.

2.6. Determination of the composition in macromolecules of biofilms

After the incubation period, and in the same manner as described in section 2.5, the surfaces were washed with 6 ml of sterile distilled water. Each coupon was subsequently stained with a staining solution containing three fluorochromes: Concanavalin A-Alexa Fluor 594 (ConA 594; ThermoFisher Scientific, Barcelona, Spain), which binds to α-mannopyranosyl and α-glucopyranosyl residues (Stiefel et al., 2016), showing up in fluorescent red; 4′, 6-diamino-2-phenylindole (DAPI, ThermoFisher Scientific, Barcelona, Spain), which has an affinity for DNA, showing up in fluorescent blue; Fluorescein-5-isothiocyanate (FITC, Sigma-Aldrich, Madrid, Spain), which has an affinity for proteins through amino groups, and specifically with the isothiocyanate group that reacts with terminal amino groups and primary amines (Chen et al., 2007), showing up in fluorescent green. To make the staining solution, 1 mg ml^{-1} of each fluorochrome was combined with 0.1 M

sodium bicarbonate (NaHCO, Panreac, Castellar del Vallès, Spain). Moreover, 10 μl of ConA, 10 μl of DAPI, and 5 μl of FITC were added to each coupon together with 75 μl of 0.1 M $NaHCO_3$. Once the 100 μl was deposited on the coupons, the samples were incubated at room temperature in dark conditions for 1 h so that the dyes could penetrate the structure. This combination has proven to be effective in studying the composition of biofilm macromolecules (Ripolles-Avila et al., 2020).

After the incubation period, the staining solution was removed from the coupons by gravity and washed with 3 ml of sterile distilled water to eliminate the remaining stain from the surface. The coupons were then evaluated by DEM. As in section 2.5, 6 different fields were taken for each sample, but with the difference that 3 photographs corresponding to 3 different filters were taken for each field, enabling the portions of the macromolecules studied in each field photographed to be distinguished. The software described in section 2.5 was again used to analyze the images, and the results were expressed as a percentage of each of the marked elements.

2.7. Qualitative evaluation of the distribution of biofilm components

This evaluation was carried out following the same methodology described in sections 2.5 and 2.6, with the difference in this case that the samples were analyzed by CLSM using a Spectal Multiphoton Leica TCS SP5 microscope (Leica Microsistemas, Barcelona, Spain). The samples, each consisting of 6 photographs, were analyzed using a 20X objective, and according to the emission of each dye. The specialized software IMARIS 7.1 (Bitplane, Zurich, Switzerland) was used to analyze the images, from which the 3D models were obtained.

2.8. Statistical methods

The tests corresponding to the evaluation by DEM and CLSM were carried out in duplicate in three different experiments (n = 6). The bacterial counts obtained by DEM were converted to decimal logarithmic values, thus coinciding with the assumption of a normal distribution. IBM SPSS Statistics version 23 was used to analyze the data statistically. The One Way Anova test, with a posterior contrast using Tukey's test, was used for the means comparison to observe if there were significant differences between the counts obtained. A $P < 0.05$ was considered as statistically significant.

3. Results and discussion

3.1. Evaluation of the mono-species biofilm formation capacity on stainless steel surfaces

Table 1 shows that the three strains evaluated showed a high capacity to form biofilms, presenting a total count of adhered cells greater than 7 log CFU cm^{-2} in all cases. To this effect, *S. aureus* turned out to be the strain with the greatest capacity to form biofilms within the group of microorganisms evaluated. An average count was significantly different ($P < 0.05$) from the others. Ibarra-Trujillo et al. (2012) also demonstrate that *S. aureus* is a highly pathogenic biofilm producer, thus supporting the results obtained in the present study where *S. aureus* was determined to be the largest biofilm producer with a total count of 7.76 ± 0.03 log CFU cm^{-2}. It is important to highlight that the type of surface is a fundamental factor that directly influences biofilm formation (Whitehead et al., 2009). Although high counts were obtained for this pathogen when using stainless steel surfaces, other authors such as Di Ciccio et al. (2015) and Poimenidou et al. (2016) indicated that *S. aureus* possesses a greater capacity to form biofilms on polystyrene than on stainless steel. However, it is known that the capacity to form biofilms among strains belonging to the same species is varied (Borges et al., 2018; Ripolles-Avila, Hascoët, et al., 2019). In this context, Jang et al. (2018) demonstrated that modifying stainless steel as a food contact material through electrochemical engravings effectively inhibits the adhesion of *S. aureus*.

Table 1
Count of cells that made up the biofilms of the studied strains, expressed in log CFU cm^{-2} and evaluated by DEM. The survival value expressed as a percentage is also shown. Each value corresponds to an average of two repetitions carried out in three different experiments (n = 6). The standard error of the mean has also been calculated.

Bacterial strains	Total count Log CFU cm^{-2}	Survival rate (%)
L. monocytogenes CECT 5672	7.56 ± 0.04^{b}	90.48 ± 1.62^{a}
S. Typhimurium CECT 4594	7.26 ± 0.03^{c}	60.31 ± 4.45^{b}
S. aureus CECT 239	7.76 ± 0.03^{a}	94.13 ± 1.77^{a}

[a-c] Values within the column that lack a common superscript differ significantly ($P < 0.05$).

In descending order, *L. monocytogenes* was next, the average count of which presented statistically significant differences ($P < 0.05$) compared with the rest. Ripolles-Avila, Cervantes-Huaman, et al. (2019) evaluated the capacity to form biofilms of 17 *L. monocytogenes* strains using DEM, resulting in the CECT 5672 strain presenting the highest count, with a similar value to the one obtained in the present study. In third and last place was *S.* Typhimurium, whose average count also presented significant differences ($P < 0.05$) compared with the rest. Overall, the results of the present study reveal that the Gram-positive bacteria used have a greater capacity for biofilm formation than Gram-negative bacteria. However, these results cannot be extrapolated to a fact dependent on the type of cell wall that the bacteria have, since biofilm formation depends on different factors, among which the generation of a protective matrix stands out, for which different metabolic pathways are used (Hassan-Muhammad et al., 2020). To discuss that, in the study conducted by Borges et al. (2018), the biofilm formation capacity of 243 strains of *Salmonella* spp. at four different incubation temperatures (37 °C, 28 °C, 12 °C and 3 °C) were evaluated. A total of 92.2% of the strains analyzed were able to produce biofilms at least one of the tested temperatures. In the tests, 71.6% of the strains produced biofilms at 37 °C, 63% at 28 °C, 52.3% at 12 °C, and 39.5% at 3 °C. It is important to emphasize the capacity of *Salmonella* spp. to produce biofilms at 3 °C (Silva et al., 2008). Piras et al. (2015) reported a higher biofilm production at 22 °C than at 35 °C. These findings indicate that the factors involved in the production of biofilms have different responses depending on the incubation temperature (Cabarkapa et al., 2015). Based on these studies and under the test conditions established in the present study, *S.* Typhimurium was expected to present higher counts, together with a better capacity to form biofilms, when incubated at 30 °C.

As Table 1 shows, the survival percentage of the generated biofilms was also measured. The proportion of viable cells in the biofilms formed by the assessed Gram-positive bacteria (*i.e. L. monocytogenes* and *S. aureus*) ranged from 90.48% to 94.13%, with the highest percentage corresponding to *S. aureus* biofilms, although with no significant differences with *L. monocytogenes* survival rate ($P = 0.91$). In contrast, *S.* Typhimurium survival rate presented significant differences ($P < 0.05$) with both Gram-positive bacteria. In this case, it is highly interesting to point out that the total cell counts of the biofilms produced by the three bacteria were around 7 logs although *S.* Typhimurium survival rate was much lower (*i.e.* 60.31%), implying therefore that approximately 40% of cells conforming *S.* Typhimurium biofilms were dead. It has been described for other Gram-negative bacteria, such as *Klebsiella pneumoniae*, that for conforming strong biofilms, eDNA as well as other matrix components appear because of increased cell death, what makes these structures stronger (Desai et al., 2019). Moreover, the fact that non-viable cell counts were obtained, which in some cases were very high, could be because with long incubation times the bacteria that form the biofilms can overcome their own exponential growth curve, reaching cell death. This not only helps to structure the system, but it also provides the cells that remain viable in the biofilm with a new source of energy (Ripolles-Avila et al., 2018). This fact has been observed in the

study of biofilms of other microorganisms such as *Bacillus subtilis*, in whose non-viable cells complex three-dimensional structures are generated. It also constitutes a stress response at the community level to improve the resistance of biofilms to unfavorable environmental conditions (Asally et al., 2012).

Fig. 1 depicts the shape of the cells that make up the various biofilms and their distribution on the surface, which is sometimes geometric and other times more distributed. In this regard, it has been suggested that the organization of the cells from which biofilms are created, as detected by DEM, can be used to predict their creation (Ripolles-Avila et al., 2018). With this in mind, it can be proven that all of the bacterial strains utilized in the study developed biofilms after a one-week incubation period, albeit with varying degrees of organization. This finding is consistent with that of Centorame et al. (2017), who found that biofilms have a more complicated organization and a larger density of connected cells after a week of incubation. Furthermore, conditioning in a humidity-saturated chamber led to the formation of mature biofilms, as also stated by Mai et al. (2006), since this is a primary determinant in the adhesion of microorganisms and a way to help them to distribute on the surface.

A characteristic that shows that a biofilm has reached its maturity stage is the presence of water channels (Bryers, 2000). These formations promote the constant circulation of nutrients and the elimination of residues within the biofilm structure (Donlan & Costerton, 2002). In Fig. 1-a and **1-b**, corresponding to *L. monocytogenes* and *S.* Typhimurium, respectively, the presence of interstitial spaces that can be assumed to be water channels was revealed. Contrarily, *S. aureus* showed dense colonization on the surface, preventing the clear visualization of these channels (Fig. 1-c), concurring with the observations of Ibarra-Trujillo et al. (2012).

3.2. Determination of the composition in macromolecules of biofilms

Fig. 2 compiles the results of the macromolecules composition evaluation. Proteins were the major component of the biofilm matrix for all of them (Fig. 2-A). The protein content of biofilms matrices formed by *L. monocytogenes*, *S.* Typhimurium, and *S. aureus* (83.35 ± 5.81%, 83.37 ± 3.35% and 82.55 ± 2.39%, respectively) did not present significant differences ($P = 0.98$) among them. Colagiorgi et al. (2016) described that *L. monocytogenes* ECM is mainly composed of proteins. Likewise, surface treatments with protease have been shown to trigger an alteration in the development of biofilms produced by *L. monocytogenes* or to induce the dispersion of the cells that form them, indicating the key role that proteins play in the development and maintenance of the structure (Nguyen & Burrows, 2014). Moormeier et al. (2014) determined that adding proteases during the cell multiplication stage cancels the formation of *S. aureus* biofilms, revealing that the formation of microcolonies and the subsequent maturation of the structure involves a component of a protein nature. Furthermore, Gonzáles-Machado et al. (2018) determine that the major component of ECM formed by *Salmonella enterica* Agona is proteins, a comparable result to the one obtained in the present study. All this supports the results obtained in the present study, where none of the pathogens showed significant differences ($P > 0.05$) in the proteins content, thus proving their role importance on biofilms integrity.

Fig. 2-B shows that *L. monocytogenes* and *S. aureus* were the strains

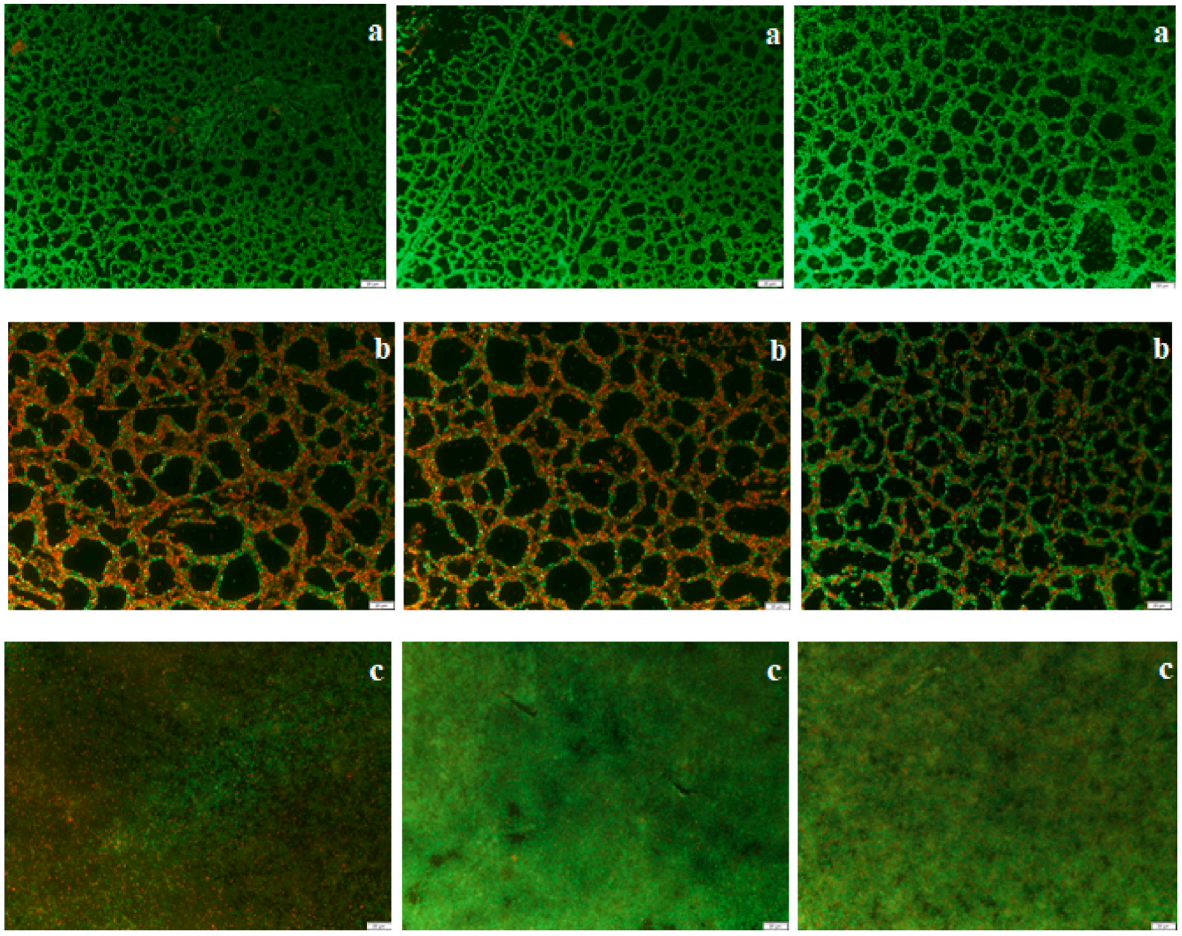

Fig. 1. DEM images of biofilms of (a) *L. monocytogenes* CECT 5672, (b) *S.* Typhimurium CECT 4594, and (c) *S. aureus* CECT 239, stained with Live/Dead Baclight. Magnification 20X.

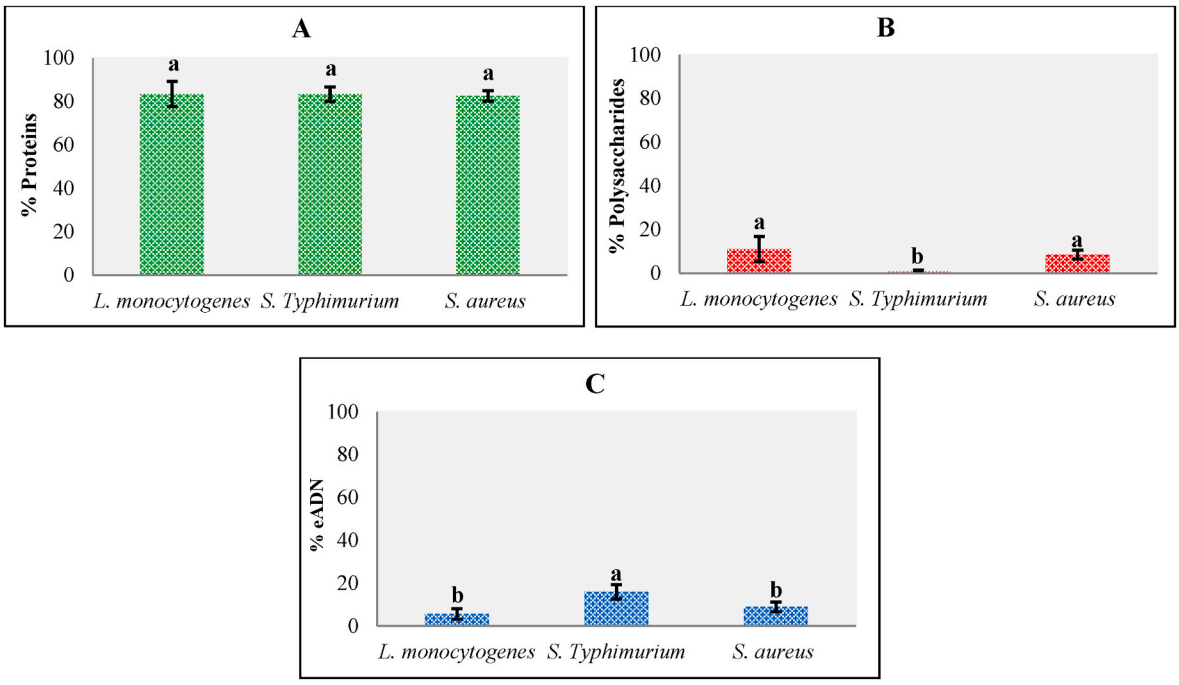

Fig. 2. Content of (A) proteins, (B) polysaccharides, and (C) eDNA, present in the matrix of biofilms formed *by L. monocytogenes* CECT 5672, *S.* Typhimurium CECT 4594, and *S. aureus* CECT 239. Data expressed in percentages. The error bars represent the standard error of the mean (n = 6). [a–b]Different letters indicate that the values differ significantly ($P < 0.05$).

that presented the highest percentage of polysaccharides in the biofilm matrix (10.98 ± 5.77% and 8.48 ± 2.07%, respectively), with no significant differences ($P = 0.54$). Contrarily, *S.* Typhimurium presented a low percentage of polysaccharides of 0.68 ± 0.77% in its matrix. The composition of the exopolysaccharides as ECM is different in each bacterium, for example, it is cellulose in *S.* Typhimurium, poly-N-acetylglucosamine in *S. aureus* (Lasa et al., 2005), and teichoic acids in *L. monocytogenes* (Brauge et al., 2016).

Last, Fig. 2-C shows that *S.* Typhimurium presented the highest percentage of eDNA in the biofilm matrix (15.95 ± 3.39%), and that this percentage was significantly different ($P < 0.05$) from those obtained for the rest of the studied strains. *L. monocytogenes* and *S. aureus* did not show significant differences ($P = 0.23$) in terms of the content of eDNA present in the biofilm matrix. Although a lower proportion of eDNA was obtained for both these pathogens, this component has been demonstrated to be an important determinant in biofilms. In this regard, Rice et al. (2007) determined that eDNA is an important structural component of the matrix of *S. aureus* biofilms. Nguyen and Burrows (2014) and Zetzmann et al. (2015) found eDNA to be a cohesive and structural matrix component for *L. monocytogenes* biofilms. Last, eDNA not only plays a structural role, but it also serves as a source of energy and nutrients (Harmsen et al., 2010).

In the present study, lipids were not included in the determination of components that conform biofilm matrix as, normally, it is composed of highly hydrated hydrophilic molecules and just, in some cases, ECM have hydrophobic properties. It seems that the most important type of lipids in terms of biofilm formation are rhamnolipids, which can be found in the matrix of *Pseudomonas aeruginosa*. Interestingly, they display surface activity and have been proposed to act in initial microcolony formation, facilitating surface-associated bacterial migration and the formation of mushroom-shaped structures, preventing colonization of channels, and playing a part in biofilm dispersion (Flemming & Wingender, 2010). However, modelized biofilms of the present study are not distinguished for producing such substances. Preliminary studies showed that fat content on *L. monocytogenes* biofilms was negligible (Ripolles-Avila et al., 2018).

At a qualitative level, the structures were similar in organization to those previously found in a cell viability study (Fig. 3). On this regard, *S. aureus* showed highest cell count, highest survivability, and highest structural density, although the composition of the biofilms matrix's macromolecules was similar to the other Gram-positive bacteria. On the contrary, polysaccharide and eDNA content was significantly different ($P < 0.05$) than *S.* Typhimurium, what can also be the reason of higher survivability. Different studies focused on enzymatic technology to eliminate biofilms have determined that its action largely depends on the biofilm-forming species, the interactions between the species that form the biofilm, and the environmental conditions. For example, Lequette et al. (2010) found that polysaccharides have a significant effect in terms of the matrix destabilization of biofilms formed with *Pseudomonas fluorescens*, while serine proteases have a greater release effect on the biofilms formed by *Bacillus* spp. (Lequette et al., 2010). Lefebvre et al. (2016) found that alpha-amylase is more effective to detach *P. aeruginosa* biofilm cells than *S. aureus* biofilm cells. This fact indicates the importance of studying the type of resident microbiota in each food industry and the matrix composition they produce. This knowledge will be useful to design and define cleaning strategies and effective disinfection and personalize industrial treatments.

3.3. Evaluation of the distribution of the components that form the biofilms

Several studies have used CLSM as a tool for the morphological and structural analysis of biofilms (Bridier et al., 2010; Ramírez-Granillo et al., 2015; Reis-Teixeira et al., 2017; Walker & Horswill, 2012), and for determining the composition in macromolecules of the biofilm matrix (Fish et al., 2017). The combination of CLSM with an image analysis system represents an important and accepted research tool for analyzing and understanding highly complex systems such as biofilms (Neu et al., 2010). There is currently no fluorescence labeling method that visualizes the biofilm matrix in general, due to the complex and highly variable composition of the matrix produced by different bacteria and under different environmental conditions (Schlafer & Meyer, 2017). For this

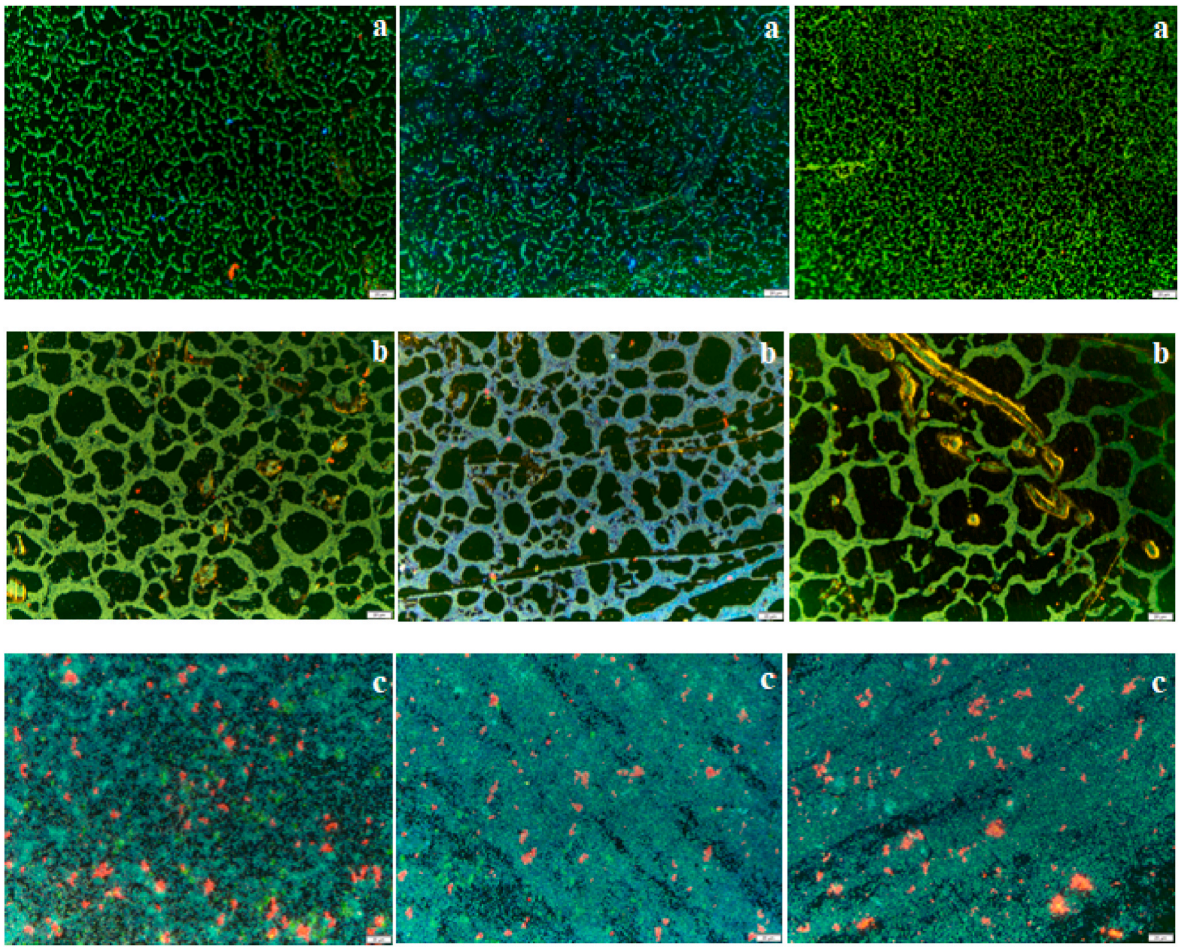

Fig. 3. DEM images of the macromolecular composition of the matrix of biofilms formed by (a) *L. monocytogenes* CECT 5672, (b) *S.* Typhimurium CECT 4594, and (c) *S. aureus* CECT 239, stained with Concanavalin A (red), FITC (green), and DAPI (blue). Magnification 20X. (For interpretation of the references to colour in this figure legend, the reader is referred to the Web version of this article.)

reason, the majority macromolecules of the biofilm matrix were individually stained. The distribution of the components within the biofilms can be observed with respect to cell viability (Fig. 4) and the majority macromolecules (Fig. 5). These figures show similar results to those observed in Figs. 1 and 2, respectively. However, there is no evidence of a homogeneous and/or ordered distribution of the elements studied within the biofilm for each case. Bridier et al. (2010) use CLSM to determine the biovolume generated in biofilms formed by various pathogens, determining that *S. aureus* has a high biovolume value, *L. monocytogenes* an intermediate value, and *S. enterica* a lower value. These findings are consistent with those of the current study, which used DEM to assess the number of cells that form biofilms (Table 1). Figs. 4a and 5a show that *L. monocytogenes* produces a thin biofilm, similar to the findings of Reis-Teixeira et al. (2017) and Bridier et al. (2010), who did not observe that *L. monocytogenes* has multiple layers and so are shown with a thin profile. This qualitative analysis of the distribution of biofilm components and architecture provides valid criteria to be considered in the design of strategies for their elimination.

4. Conclusions

L. monocytogenes CECT 5672, *S.* Typhimurium CECT 4594, and *S. aureus* CECT 239 showed great biofilm forming capacity on stainless steel surfaces under the established experimental conditions, based on both the number of cells that form the biofilms and the structure generated. Among them, *S. aureus* was shown to be the pathogen with the highest cell count, highest survival, and highest structural density. Regarding the composition in macromolecules of the matrix, all the species obtained a higher percentage of proteins. However, the composition of polysaccharides and eDNA differed between the strains studied. Last, the 3D representations of the produced biofilms did not show a homogeneous and/or ordered distribution of their components (viable and non-viable cells, proteins, polysaccharides, and eDNA). This quantitative determination of the majority macromolecules that form the biofilm matrix and the analysis of their qualitative characteristics represents an advance for the development of new products and the design of possible strategies for their elimination.

Declaration of interest

The authors declare no conflict of interest.

Funding sources

This study was supported by Research Project grants RTI2018-098267-R-C32 from the Ministerio de Ciencia, Innovación y Universidades.

CRediT authorship contribution statement

B.R.H. Cervantes-Huamán: Conceptualization, Methodology, Formal analysis, Investigation, Writing – original draft. **C. Ripolles-Avila:** Conceptualization, Methodology, Validation, Writing – review & editing, Supervision. **T. Mazaheri:** Methodology, Investigation. **J.J.**

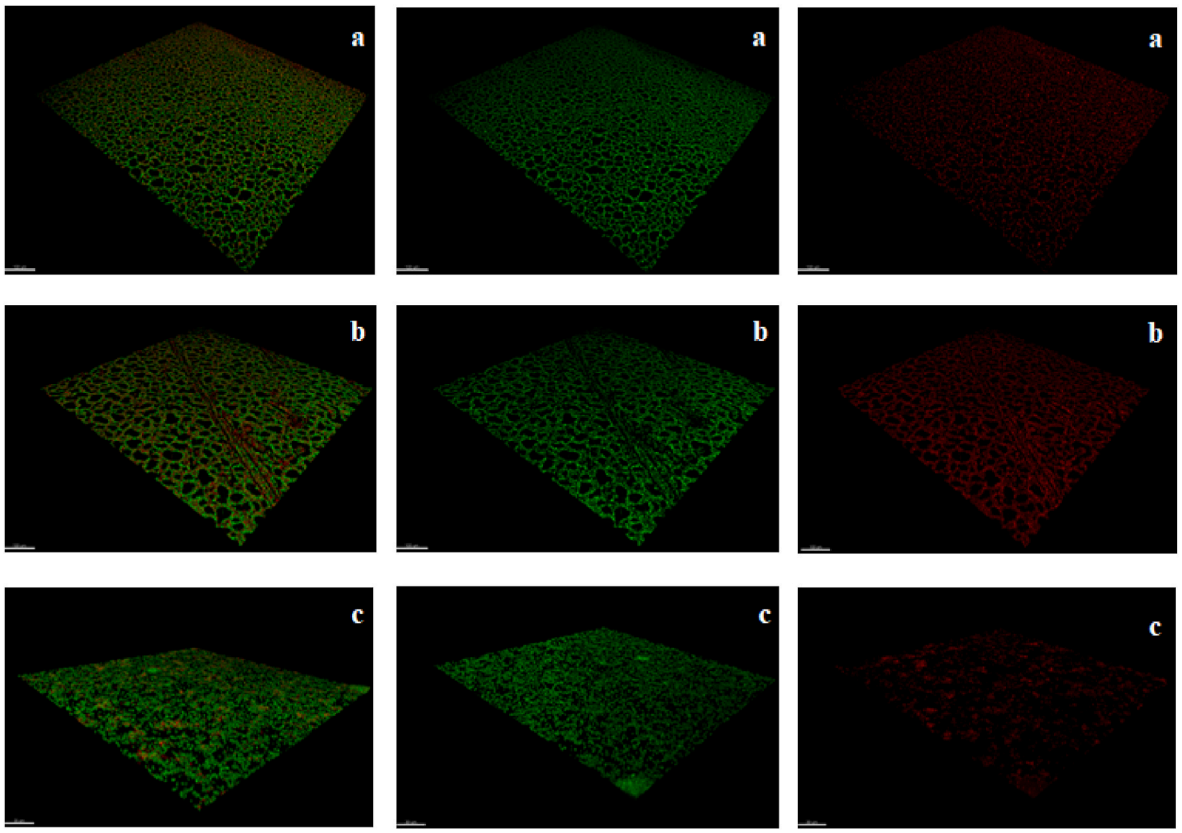

Fig. 4. 3D images obtained by CLSM of the biofilms formed by (a) *L. monocytogenes* CECT 5672, (b) *S*. Typhimurium CECT 4594, and (c) *S. aureus* CECT 239, stained with Live/Dead Baclight. Viable cells are marked in green and non-viable cells in red. The second column represents only living cells and the second column only deaths. Magnification 20X. (For interpretation of the references to colour in this figure legend, the reader is referred to the Web version of this article.)

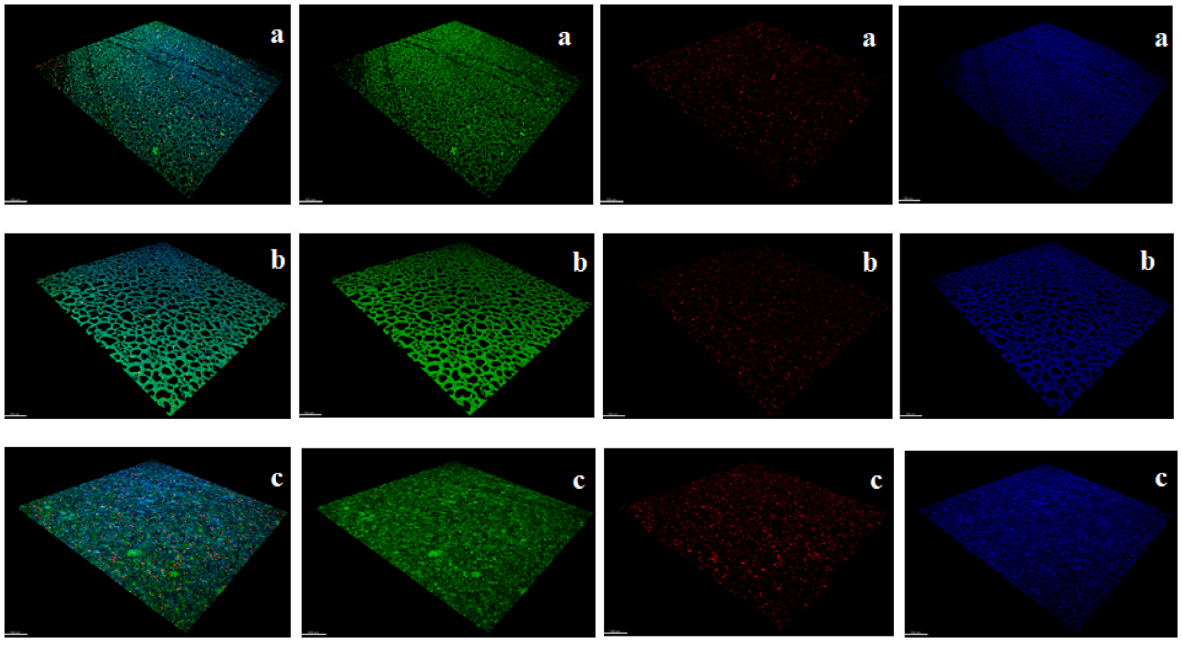

Fig. 5. 3D images obtained by CLSM of the biofilms formed by (a) *L. monocytogenes* CECT 5672, (b) *S*. Typhimurium CECT 4594, and (c) *S. aureus* CECT 239, stained with Concanavalin A (red) which marks polysaccharides, FITC (green) which marks proteins, and DAPI (blue) which marks eDNA. The second column represents only proteins, the third only polysaccharides, and the fourth only eDNA. Magnification 20X.

Rodríguez-Jerez: Conceptualization, Validation, Writing – review & editing, Supervision, Project administration, Funding acquisition.

Acknowledgements

The authors thank Judit, Helena, and Nuria from the Microscopy

Service of the UAB for their for her technical support in CLSM. The authors alone are responsible for the content and writing of the paper. The authors acknowledge Ms. Sarah Davies for the English grammar review.

References

AENOR. (2015). *ISO 13697. Antisépticos y desinfectantes químicos. Ensayo cuantitativo de superficie no porosa para la evaluación de la actividad bactericida y/o fungicida de los desinfectantes químicos utilizados en productos alimenticios, en la industria, en el hogar y en colectividades*.

Asally, M., Kittisopikul, M., Rue, P., Du, Y., Hu, Z., Cagatay, T., & Süel, G. M. (2012). Localized cell death focuses mechanical forces during 3D patterning in a biofilm. *Proceedings of the National Academy of Sciences, 109*(46), 18891–18896. https://doi.org/10.1073/pnas.1212429109

Borges, K. A., Furian, T. Q., Souza, S. N., Menezes, R., Tondo, E. C., Salle, C. T. P., Moraes, H. L. S., & Nascimento, V. P. (2018). Biofilm formation capacity of *Salmonella* serotypes at different temperature conditions. *Pesquisa Veterinária Brasileira, 38*(1), 71–76. https://doi.org/10.1590/1678-5150-pvb-4928

Branda, S. S., Vik, S., Friedman, L., & Kolter, R. (2005). Biofilms: The matrix revisited. *Trends in Microbiology, 13*, 20–26. https://doi.org/10.1016/j.tim.2004.11.006

Brauge, T., Sadovskaya, I., Faille, C., Benezech, T., Maes, E., Guerardel, Y., & Midelet-Bourdin, G. (2016). Teichoic acid is the major polysaccharide present in the *Listeria monocytogenes* biofilm matrix. *FEMS Microbiology Letters, 363*(2), Article fnv229. https://doi.org/10.1093/femsle/fnv229

Bridier, A., Dubois-Brissonnet, F., Boubetra, A., Thomas, V., & Briandet, R. (2010). The biofilm architecture of sixty opportunistic pathogens deciphered using a high throughput CLSM method. *Journal of Microbiological Methods, 82*(1), 64–70. https://doi.org/10.1016/j.mimet.2010.04.006

Bryers, J. D. (2000). Biofilm formation and persistence. In J. D. Bryers (Ed.), *Biofilms II: Process analysis and applications* (pp. 45–88). New York: Wiley-Liss Inc.

Cabarkapa, I., Skrinjar, M., Levic, J., Kokic, B., Blagojev, N., Milanov, D., & Suvajdzic, L. (2015). Biofilm forming ability of *Salmonella enteritidis* in vitro. *Acta Veterinaria Brno, 65*(3), 371–389. https://doi.org/10.1515/acve-2015-0031

Carpentier, B., & Cerf, O. (2011). Review - persistence of *Listeria monocytogenes* in food industry equipment and premises. *International Journal of Food Microbiology, 145*, 1–8. https://doi.org/10.1016/j.ijfoodmicro.2011.01.005

Castro-Rosas, J., & Escartín, E. F. (2005). Increased tolerance of *Vibrio cholerae* O1 to temperature, pH, or drying associated with colonization of shrimp carapaces. *International Journal of Food Microbiology, 102*, 195–201. https://doi.org/10.1016/j.ijfoodmicro.2004.12.015

Centorame, P., D'Angelo, A. R., Di Simone, F., Salini, R., Cornacchia, A., Marrone, R., & Pomilio, F. (2017). *Listeria monocytogenes* biofilm production on food packaging materials submitted to physical treatment. *Italian Journal of Food Safety, 6*(3), 106–109. https://doi.org/10.4081/ijfs.2017.6654

Chen, M. Y., Lee, D. J., Tay, J. H., & Show, K. Y. (2007). Staining of extracellular polymeric substances and cells in bioaggregates. *Applied Microbiology and Biotechnology, 75*(2), 467–474. https://doi.org/10.1007/s00253-006-0816-5

Colagiorgi, A., Di Ciccio, P., Zanardi, E., Ghidini, S., & Ianieri, A. (2016). A look inside the *Listeria monocytogenes* biofilms extracellular matrix. *Microorganisms, 4*(22), 1–12. https://doi.org/10.3390/microorganisms4030022

Coughlan, L. M., Cotter, P. D., Hill, C., & Alvarez-Ordóñez, A. (2016). New weapons to fight old enemies: Novel strategies for the (bio) control of bacterial biofilms in the food industry. *Frontiers in Microbiology, 7*, 1–21. https://doi.org/10.3389/fmicb.2016.01641

Dantas, S. T. A., Rossi, B. F., Bonsaglia, E. C. R., Castilho, I. G., Hernandes, R. T., Fernandes, A., & Rall, V. L. M. (2018). Cross-contamination and biofilm formation by *Salmonella enterica* serovar Enteritidis on various cutting boards. *Foodborne Pathogens and Disease, 15*, 81–85. https://doi.org/10.1089/fpd.2017.2341

Desai, S., Sanghrajka, K., & Gajjar, D. (2019). High adhesion and increased cell death contribute to strong biofilm formation in *Klebsiella pneumoniae*. *Pathogens, 8*(4), 1–16. https://doi.org/10.3390/pathogens8040277

Di Ciccio, P., Vergara, A., Festino, A. R., Paludi, D., Zanardi, E., Ghidini, S., & Ianieri, A. (2015). biofilm formation by *Staphylococcus aureus* on food contact surfaces: Relationship with temperature and cell surface hydrophobicity. *Food Control, 50*, 930–936. https://doi.org/10.1016/j.foodcont.2014.10.048

Donlan, R., & Costerton, J. (2002). Biofilms: Survival mechanisms of clinically relevant microorganisms. *Clinical Microbiology Reviews, 15*(2), 167–193. https://doi.org/10.1128/CMR.15.2.167-193.2002

Fish, K., Osborn, A. M., & Boxall, J. B. (2017). Biofilm structures (EPS and bacterial communities) in drinking water distribution systems are conditioned by hydraulics and influence discolouration. *The Science of the Total Environment, 593–594*, 571–580. https://doi.org/10.1016/j.scitotenv.2017.03.176

Flemming, H., & Wingender, J. (2010). The biofilm matrix. *Nature Reviews Microbiology, 8*(9), 623–633. https://doi.org/10.1038/nrmicro2415

Fuster-Valls, N., Hernández-Herrero, M., Marín-de-Mateo, M., & Rodríguez-Jerez, J. J. (2008). Effect of different environmental conditions on the bacteria survival on stainless steel surfaces. *Food Control, 19*(3), 308–314. https://doi.org/10.1016/j.foodcont.2007.04.013

González-Machado, C., Capita, R., Riesco-Peláez, F., & Alonso-Calleja, C. (2018). Visualization and quantification of the cellular and extracellular components of *Salmonella* Agona biofilms at different stages of development. *PLoS One, 13*(7). https://doi.org/10.1371/journal.pone.0200011

González-Rivas, F., Ripolles-Avila, C., Fontecha-Umaña, F., Ríos-Castillo, A. G., & Rodríguez-Jerez, J. J. (2018). Biofilms in the spotlight: Detection, quantification, and removal methods. *Comprehensive Reviews in Food Science and Food Safety, 17*(5), 1261–1276. https://doi.org/10.1111/1541-4337.12378

Harmsen, M., Lappann, M., Knøchel, S., & Molin, S. (2010). Role of extracellular DNA during biofilm formation by *Listeria monocytogenes*. *Applied and Environmental Microbiology, 76*(7), 2271–2279. https://doi.org/10.1128/AEM.02361-09

Hyde, J., Darouiche, R., & Costerton, J. (1998). Strategies for prophylaxis against prosthetic valve endocarditis: A review article. *Journal of Heart Valve Disease, 7*(3), 316–326. Retrieved from https://www.ncbi.nlm.nih.gov/pubmed/9651846.

Ibarra-Trujillo, C., Villar-Vidal, M., Gaitán-Cepeda, L. A., Pozos-Guillen, A., Mendoza-de Elias, R., & Sánchez-Vargas, L. O. (2012). Ensayo de formación y cuantificación de biopelículas mixtas de *Candida albicans* y *Staphylococcus aureus*. *Revista Iberoamericana De Micologia, 29*(4), 214–222. https://doi.org/10.1016/j.riam.2012.02.003

Jahid, I. K., & Ha, S. (2012). A review of microbial biofilms of produce: Future challenge to food safety. *Food Science Biotechnology, 21*, 299–316. https://doi.org/10.1007/s10068-012-0041-1

Jang, Y., Choi, W. T., Johnson, C. T., García, A. J., Singh, P. M., Breedveld, V., & Champion, J. A. (2018). Inhibition of bacterial adhesion on nanotextured stainless steel 316L by electrochemical etching. *ACS Biomaterials Science & Engineering, 4*(1), 90–97. https://doi.org/10.1021/acsbiomaterials.7b00544

Lasa, I., Del Pozo, J. L., Penadés, J. R., & Leiva, J. (2005). Bacterial biofilms and infection. *Anales del Sistema Sanitario de Navarra, 28*(2), 163–175. Retrieved from http://scielo.isciii.es/scielo.php?script=sci_arttext&pid=S1137-66272005000300002.

Lefebvre, E., Vighetto, C., Di Martino, P., Larreta-Garde, V., & Seyer, D. (2016). Synergistic antibiofilm efficacy of various commercial antiseptics, enzymes and EDTA: A study of *Pseudomonas aeruginosa* and *Staphylococcus aureus* biofilms. *International Journal of Antimicrobial Agents, 48*(2), 181–188. https://doi.org/10.1016/j.ijantimicag.2016.05.008

Lequette, Y., Boels, G., Clarisse, M., & Faille, C. (2010). Using enzymes to remove biofilms of bacterial isolates sampled in the food-industry. *Biofouling, 26*(4), 421–431. https://doi.org/10.1080/08927011003699535

Mai, T. L., Sofyan, N. I., Fergus, J. W., Gale, W. F., & Conner, D. E. (2006). Attachment of *Listeria monocytogenes* to an austenitic stainless steel after welding and accelerated corrosion treatments. *Journal of Food Protection, 69*(7), 1527–1532. https://doi.org/10.4315/0362-028X-69.7.1527

Mazaheri, T., Ripolles-Avila, C., Hascoët, A. S., & Rodríguez-Jerez, J. J. (2020). Effect of an enzymatic treatment on the removal of mature *Listeria monocytogenes* biofilms: A quantitative and qualitative study. *Food Control, 114*, Article 107266. https://doi.org/10.1016/j.foodcont.2020.107266

Meireles, A., Borges, A., Giaouris, E., & Simões, M. (2016). The current knowledge on the application of antibiofilm enzymes in the food industry. *Food Research International, 86*, 140–146. https://doi.org/10.1016/j.foodres.2016.06.006

Moormeier, D. E., Bose, J. L., Horswill, A. R., & Bayles, K. W. (2014). Temporal and stochastic control of *Staphylococcus aureus* biofilm development. *mBio, 5*(5), e01341–14. https://doi.org/10.1128/mBio.01341-14

Møretrø, T., Langsrud, S., & Heir, E. (2013). Bacteria on meat abattoir process surfaces after sanitation: Characterisation of survival properties of *Listeria monocytogenes* and the commensal bacterial flora. *Advances in Microbiology, 3*, 255–264. https://doi.org/10.4236/aim.2013.33037

Muhammad, M. H., Idris, A. L., Fan, X., Guo, Y., Yu, Y., Jin, X., & Huang, T. (2020). Beyond risk: Bacterial biofilms and their regulating approaches. *Frontiers in Microbiology, 11*(May), 1–20. https://doi.org/10.3389/fmicb.2020.00928

Neu, T. R., Manz, B., Volke, F., Dynes, J. J., Hitchcock, A. P., & Lawrence, J. R. (2010). Advanced imaging techniques for assessment of structure, composition and function in biofilm systems. *FEMS Microbiology Ecology, 72*(1), 1–21. https://doi.org/10.1111/j.1574-6941.2010.00837.x

Nguyen, U. T., & Burrows, L. L. (2014). DNase I and proteinase K impair *Listeria monocytogenes* biofilm formation and induce dispersal of pre-existing biofilms. *International Journal of Food Microbiology, 187*, 26–32. https://doi.org/10.1016/j.ijfoodmicro.2014.06.025

OMS. (2015). *Informe de la OMS señala que los niños menores de 5 años representan casi un tercio de las muertes por enfermedades de transmisión alimentaria*.

Piras, F., Fois, F., Consolati, S. G., Mazza, R., & Mazzette, R. (2015). Influence of temperature, source, and serotype on biofilm formation of *Salmonella enterica* isolates from pig slaughterhouses. *International Association for Food Protection, 78*(10), 1875–1878. https://doi.org/10.4315/0362-028X.JFP-15-085

Poimenidou, S. V., Chrysadakou, M., Tzakoniati, A., Bikouli, V. C., Nychas, J. J., & Skandamis, P. N. (2016). Variability of *Listeria monocytogenes* strains in biofilm formation on stainless steel and polystyrene materials and resistance to peracetic acid and quaternary ammonium compounds. *International Journal of Food Microbiology, 237*, 164–171. https://doi.org/10.1016/j.ijfoodmicro.2016.08.029

Ramadan, H. H. (2006). Chronic rhinosinusitis and bacterial biofilms. *Current Opinion in Otolaryngology & Head and Neck Surgery, 14*(3), 183–186. https://doi.org/10.1097/01.moo.0000193177.62074.fd

Ramírez-Granillo, A., Canales, M. G., Espíndola, M. E., Martínez-Rivera, M. A., de Lucio, V. M., & Tovar, A. V. (2015). Antibiosis interaction of *Staphylococccus aureus* on *Aspergillus fumigatus* assessed in vitro by mixed biofilm formation. *BMC Microbiology, 15*, 33. https://doi.org/10.1186/s12866-015-0363-2

Reis-Teixeira, F. B. dos, Alves, V. F., & Martinis, E. C. P. de (2017). Growth, viability and architecture of biofilms of *Listeria monocytogenes* formed on abiotic surfaces. *Brazilian Journal of Microbiology, 48*, 587–591. https://doi.org/10.1016/j.bjm.2017.01.004

Rice, K. C., Mann, E. E., Endres, J. L., Weiss, E. C., Cassat, J. E., Smeltzer, M. S., & Bayles, K. W. (2007). The cidA murein hydrolase regulator contributes to DNA release and biofilm development in *Staphylococcus aureus*. *Proceedings of the National Academy of Sciences of the United States of America, 104*(19), 8113–8118. https://doi.org/10.1073/pnas.0610226104

Ripolles-Avila, C., Cervantes-Huaman, B. H., Hascoët, A. S., Yuste, J., & Rodríguez-Jerez, J. J. (2019). Quantification of mature *Listeria monocytogenes* biofilm cells formed by an *in vitro* model: A comparison of different methods. *International Journal of Food Microbiology, 289*, 209–214. https://doi.org/10.1016/j.ijfoodmicro.2018.10.020

Ripolles-Avila, C., Hascoët, A. S., Guerrero-Navarro, A. E., & Rodríguez-Jerez, J. J. (2018a). Establishment of incubation conditions to optimize the *in vitro* formation of mature *Listeria monocytogenes* biofilms on food-contact surfaces. *Food Control, 92*, 240–248. https://doi.org/10.1016/j.foodcont.2018.04.054

Ripolles-Avila, C., Hascoët, A. S., Martínez-Suárez, J. V., Capita, R., & Rodríguez-Jerez, J. J. (2019). Evaluation of the microbiological contamination of food processing environments through implementing surface sensors in an Iberian pork processing plant: An approach towards the control of. *Listeria monocytogenes. Food Control, 99*, 40–47. https://doi.org/10.1016/j.foodcont.2018.12.013

Ripolles-Avila, C., Ramos-Rubio, M., Hascoët, A. S., Castillo, M., & Rodríguez-Jerez, J. J. (2020). New approach for the removal of mature biofilms formed by wild strains of *Listeria monocytogenes* isolated from food contact surfaces in an Iberian pig processing plant. *International Journal of Food Microbiology, 323*, Article 108595. https://doi.org/10.1016/j.ijfoodmicro.2020.108595

Ripolles-Avila, C., Ríos-Castillo, A. G., Fontecha-Umaña, F., & Rodríguez-Jerez, J. J. (2019). Removal of *Salmonella enterica* serovar Typhimurium and *Cronobacter sakazakii* biofilms from food contact surfaces through enzymatic catalysis. *Journal of Food Safety, 40*, Article e12755. https://doi.org/10.1111/jfs.12755

Schlafer, S., & Meyer, R. L. (2017). Confocal microscopy imaging of the biofilm matrix. *Journal of Microbiological Methods, 138*, 50–59. https://doi.org/10.1016/j.mimet.2016.03.002

Silva, D. L., Celidonio, F. A., & Oliveira, K. M. P. (2008). Verificação da temperatura de refrigeradores domésticos para minimizar a deterioração e possíveis doenças veiculadas por alimentos. *Revista Higiene Alimentar, 22*(164), 42–45. Retrieved from https://pesquisa.bvsalud.org/bvs-vet/resource/pt/vti-45357.

Speranza, B., Monacis, N., Sinigaglia, M., & Corbo, M. (2016). Approaches to removal and killing of *Salmonella* spp. biofilms. *Journal of Food Processing and Preservation, 41*(1), Article e12758. https://doi.org/10.1111/jfpp.12758

Srey, S., Jahid, I., & Ha, S. D. (2013). biofilm formation in food industries: A food safety concern. *Food Control, 31*(2), 572–585. https://doi.org/10.1016/j.foodcont.2012.12.001

Stiefel, P., Mauerhofer, S., Schneider, J., Maniura-Weber, K., Rosenberg, U., & Ren, Q. (2016a). Enzymes enhance biofilm removal efficiency of cleaners. *Antimicrobial Agents and Chemotherapy, 60*(6), 3647–3652. https://doi.org/10.1128/AAC.00400-16

Terry, A., Curtis, E., Pantle, R., & Penny, S. A. (2003). Boundaries for biofilm formation: Humidity and temperature. *Applied and Environmental Microbiology, 69*(8), 5006–5010. https://doi.org/10.1128/AEM.69.8.5006–5010.2003

Walker, J. N., & Horswill, A. R. (2012). A coverslip-based technique for evaluating *Staphylococcus aureus* biofilm formation on human plasma. *Frontiers in Cellular and Infection Microbiology, 2*, 39. https://doi.org/10.3389/fcimb.2012.00039

Whitehead, K. A., Benson, P., Smith, L. A., & Verran, J. (2009). The use of physicochemical methods to detect organic food soils on stainless steel surfaces. Biofouling. *The Journal of Bioadhesion and Biofilm Research, 25*(8), 749–756. https://doi.org/10.1080/08927010903161299

Zetzmann, M., Okshevsky, M., Endres, J., Sedlag, A., Caccia, N., Auchter, M., Waidmann, M. S., Desvaux, M., Meyer, R. L., & Riedel, C. U. (2015). DNase-sensitive and -resistant modes of biofilm formation by *Listeria monocytogenes*. *Frontiers in Microbiology, 6*(DEC), 1–11. https://doi.org/10.3389/fmicb.2015.01428